Critical parameters governing elastocaloric effect in polyisoprene rubbers for solid-state cooling

Hiba Haissoune, Gildas Coativy, Laurent Chazeau, Laurent Lebrun, Sebald Gael, Jean-Marc Chenal

Critical parameters governing elastocaloric effect in polyisoprene rubbers for solid-state cooling

Hiba Haissoune[a,b], Gildas Coativy[a], Laurent Chazeau[b], Laurent Lebrun[a] , Gael Sebald[c], Jean-Marc Chenal[b],

[a]Univ Lyon, INSA Lyon, LGEF, EA682, F69621, Villeurbanne, France

[b]Univ Lyon, INSA Lyon, Université Claude Bernard Lyon 1, CNRS, MATEIS, UMR 5510, F69621, Villeurbanne, France

[c]ELyTMaX IRL3757, CNRS, Univ Lyon, INSA Lyon, Centrale Lyon, Université Claude Bernard Lyon 1, Tohoku University, Sendai, Japan

corresponding author : Gildas Coativy email address : gildas.coativy@insa-lyon.fr

Abstract

The aim of this work is to study the critical parameters governing the eCe (elastocaloric effect) of poly-isoprene rubber (NR and IR) in use conditions of a cooling device, i.e. under partial cyclic loading. The effect of mechanical cyclic loading parameters (pre-extension ratio, waveform and frequency) on eCe was first studied. It shows that the eCe increases when the mimimum pre-extension ratio is increased and frequency is lowered from 1Hz to 0.001Hz, as it promotes strain-induced crystallization. However, it also leads to a decrease in potential cooling power, from 7 to 0.01 MW/m^3 (i.e. 8 kW/kg to 0.01 kW/kg). At intermediate frequency (f≈0.1 Hz), the comparison of square and triangular waveforms demonstrated that the former enables greater temperature variation. This is due to its holding step (at maximum extension ratio), which maximizes crystallization but also promotes stress relaxation, resulting in increased mechanical losses. Consequently, the square and triangular loadings have a COP_{mat} of 12 and 25, with a temperature variation of 4.2K and 3.6K, respectively. Regarding the formulation, rubbers that do not have a great tendency to crystallise such as synthetic polyisoprene rubber seem to have the best COP_{mat}, while to maximise ΔT, the best of our formulations are NR crosslinked with sulphur and having a crosslink density close to 1.5×10^{-4} mol/cm^3, which combine large strain induced crystallisation and entropic elasticity. This material has a COP_{mat} of about 27 and allows a ΔT≈4K, i.e.performance comparable to that of the best Shape Memory Alloys (at equivalent COP_{mat}).

1. Introduction

Solid refrigeration is an alternative technology to refrigeration systems using gases responsible for environmental issues. It involves caloric materials that can display a temperature variation induced by phase transformation due to the application of an electric field, a magnetic field or mechanical stress[1,2]. Among them, elastocaloric materials present a mechanical stress dependent phase transformation. Natural (NR) and synthetic (SR) polyisoprene rubber belong to this class of materials, their elastocaloric behavior is linked to entropic elasticity and reinforced by the strain induced crystallization phenomenon (SIC) [3–5]. They have a significant elastocaloric effect (eCe) with a temperature variation up to 14°C [6–11] and the advantages of being non-toxic, inexpensive, relatively abundant, and bio-sourced in the case of NR. Besides, in comparison with shape memory alloys (SMA), polyisoprene rubbers require low stresses (10-20 MPa for true stress) and high extension ratios (λ) (around 6), to reach a significant eCe [12] as other elastomers [13–16]. This hinders the development of solid regenerative refrigeration systems involving cyclic circulation of a fluid, in particular because such extension ratio makes difficult to ensure the device sealing and proper heat exchanges due to the large variations of heat transfer contact areas[17,18]. One way to overcome this problem is to stretch the material over a restraint and wisely chosen extensions domain range (i.e. λ_{min}=4 to λ_{max}=6) since it minimizes the material surface ($S \sim S_0 * \sqrt{\lambda}$) and thickness ($t \sim \frac{t_0}{\sqrt{\lambda}}$) variations. Moreover to maximize the eCe and improve their fatigue strength, it is necessary that the in use extension ratio domain remains in the SIC domain, i.e. with extension ratios typically greater than λ=3 for materials used near room temperature[19,20]. Nevertheless crystallization and melting of polyisoprene rubber depend on the applied thermo-mechanical loading [21,22]. Thus, it is difficult on the basis of usual tensile tests (uniaxial testing from λ=1 to λ=6 under quasi-static conditions) [22–24] to predict what will be their ability to crystallize, their mechanical properties and thus their elastocaloric power during cyclic loading without full unloading (i.e. for λ remaining above 3) [21,25].To our knowledge, no study in the literature focused on the optimization of mechanical cycling to maximize eCe in use conditions suitable for solid-state cooling device. This paper is the first devoted to the study of the influence on eCe of different characteristic parameters of cyclic non-sinusoidal loadings (pre-extension ratio, square or triangular shape, amplitude and frequency). Indeed, although the influence of frequency on the mechanical response of the sinusoidal waveform has been extensively studied, the square and triangular waveforms have not and may be potentially different due to strain-

induced crystallization phenomenon which has a nucleation time (of around 100ms) neighboring the strain time involved in use conditions of cooling device. This will be performed with a specific NR sample already studied in a previous study [10]. Besides, the ability to crystallize of polyisoprene rubber materials depends on their natural or synthetic origin [26,27], and their cross-linking density [3,28–31]. Hence we will study the impact of these different parameters in conditions close to those used in the first regenerative solid state refrigeration systems involving NR [17,18].

2. Materials and methods

The rubbers chosen for this study are Natural Rubber (NR: RSS1 purchased from Resinex) and Synthetic polyisoprene Rubber (SR : Nipol® IR2200 kindely provided by Zeon Chemical). Their formulations, processing temperatures and curing times are summarized in Table 1. The subscripts S and P refer to the crosslinking with sulfur and peroxide respectively. Samples crosslinking with sulfur samples were cured at 160°C for 14 minutes. The numbers 1.46 and 1.1 refer to their elastically active chain density obtained by swelling in toluene, which are $1.46*10^{-4}$ mol.cm^{-3} and $1.1*10^{-4}$ mol.cm^{-3} respectively (table.1). $NR_{S\_1.53}$ is also a sulfur cured natural rubber, it is a commercial grade purchased to Xinyinte Rubber Products Co., Ltd., China. The samples (NR and SR) crosslinked with peroxide were cured at 160°C for 30 minutes. $SRP_{\_1.55}$ and $NRP_{\_1.50}$ were eliminated from the study because they had a too low extension ratio at break (i.e. lower than $\lambda<4$) to be relevant.

The homemade tensile test bench used for this study allows to achieve a strain rate of 13 s^{-1}. It is equipped with a force sensor XFTC300-200N (Measurement Specialties, France) and a laser optical displacement sensor ILD1420-200 (micro-epsilon, France). In this study, the mechanical results are presented using engineering stress and extension ratio. Extension ratio, λ, is defined as $\frac{l(t)}{l_o}$ with l(t) the length at time t and l_0 the initial length. The sample tested is a parallelepiped with 1x20x20 mm^3 dimensions. The material's surface temperature is measured using a thermal camera Optris PI450 (Optris, Germany).

Table.1 Samples recipes and network chain density estimated from swelling measurements via Flory-Rhener equation [32] and Mooney Rivlin measurements [33] (*Anti-oxydant, **Stearic acid,***N-Cyclohexyl-2-benzothiazole sulfonamide,****Arcos Organics Dicumyl peroxide 99%)

Materials	**$NR_{S\_1.53}$**	**$NR_{S\_1.46}$**	**$NR_{S\_1.1}$**	**$NR_{p\_0.84}$**	**$NR_{P\_1.50}$**	**$SR_{p\_0.92}$**	**$SR_{p\_1.55}$**
NR (phr)	N/A	100	100	100	100		
SR (phr)						100	100
6PPD*(phr)	N/A	3	3	3	3	3	3
SA** (phr)	N/A	2	2				
ZnO (phr)	N/A	1.5	1.5				
CBS*** (phr)	N/A	1.9	1.27				
Sulfur (phr)	N/A	1.2	0.8				
DCP**** (phr)				1	2	1	2
$\nu_{Mooney-Rivlin}$ ($*10^{-4}$ mol.cm^{-3})	2.2	1.9	1.6	1.1	1.7	1.3	2
$\nu_{swelling}$ ($*10^{-4}$ mol.cm^{-3})	1.53	1.46	1.1	0.84	1.5	0.92	1.55
Curing time (min)	N/A	14	14	30	30	30	30
Temperature (°C)	N/A	160	160	160	160	160	160

3. Results and discussion

$NRS_{\_1.46}$ was first studied under square cyclic loading with an extension ratio amplitude $\Delta\lambda=2$ and different minimum extension ratio $\lambda_{min} \in [2,3,3.5,4]$ at f=0.005 Hz. As shown in Figure 1a, the test protocol for square cyclic loading is made of 4 steps: stretching at 13 s^{-1} from λ_{min} to $\lambda_{max}= \lambda_{min}+ \Delta\lambda$ in 150 ms, which is in the same range than the characteristic time of crystallization [34–36], a holding step during which the sample is maintained at λ_{max} for a duration of 1/(2f) which allows the material to crystallize, a fast unloading to λ_{min} and finally a holding step at constant λ_{min} for the same duration 1/(2f). As shown in figure 1b, this is reflected in the rise of the material temperature by ΔT_1 during the loading phase. During the holding step, the temperature drops as heat is transferred from the material to its surrounding. A negative temperature variation ΔT_2 is measured during the fast unloading phase, followed by a return to the initial temperature. ΔT_2 is only -1.1°C for $\lambda_{min}= 2$ (and therefore $\lambda_{max}=4$) and its origin is ascribed to entropic elasticity (stretching/unstretching of polymer chains) since during the cycle, λ_{max} is below the onset of strain induced crystallization (known to be above 4) [10,22,36]. $|\Delta T_2|$ increases strongly with the increase of λ_{min}. It is worth noting that the plotted values are the stabilized ones (i.e. obtained for the third or following cycles). Indeed, as discussed in the

supplementary section S.1 and S.2, the first cycle leads to quite different behavior due to the fact that the first loading step is performed on an amorphous sample. The much larger value of ΔT_2 for cycles with λ_{max} above 4 is explained by the melting of crystallites formed during the stretching step, which is in addition to the entropic elasticity contribution. For cycles with λ_{min}=4, ΔT_2 reaches -5.2°C. The associated crystallinity variation $\Delta\chi$ is estimated to be -10% (Supporting information S2 and S3), and explains a temperature variation of -3.4°C (calculated as $\Delta\chi.h_f$ / C_m, taking a melting enthalpy h_f =64 kJ/kg and a specific heat capacity of C_m=1,9 kJ/kg/K). Thus, SIC enables to more than double the temperature variation. This also means that the entropic elasticity contribution is not negligible. It is worth noting that, as expected, ΔT_2 is significantly smaller (in absolute value) than in the case of a full cycle, i.e. for $1<\lambda<6$ (for which $\Delta T_2 \approx$-10°C, see Supporting information Figure.S4)[10,22,37] since the melting of the crystallites is only partial: λ staying above λ_{melt}=3, the unloading step does not enable complete melting (Supporting S2).[21].

Figure 1c shows the corresponding stress-extension ratio curves. For λ_{min}=2, a quasi-elastic behavior is observed, the mechanical hysteresis, ascribed to a weak viscoelasticity, being very small (ΔW=0.14 MJ/m^3). There is no significant difference between the first and following cycles. When λ_{min} is higher than 3, the stress increases much more rapidly during stretching and reaches up to 3.3 MPa for λ_{min}=4 (λ_{max} is then equal to 6). For these λ_{min}, the presented cycle corresponds to the third and following cycles, which show less mechanical hysteresis than the first cycle, a lower stress level at λ_{min} and more hardening at λ_{max}, as discussed in supplementary sections S1 and S.2. During the holding step, a stress relaxation is observed for λ_{max} above 4 (it is negligible for λ_{max} below). This stress relaxation increases with the increase of λ_{max}: indeed, during this step, the crystallized chain portion oriented in the stretching direction gives frees up space to the remaining amorphous chain portion, lowering the stress on the chain [10,38,39]. The result is an increase in mechanical hysteresis (up to 1.1 MJ/m3). Different studies show that the mechanical hysteresis in crosslinked natural rubber (with crosslinking densities such as the ones we used) can be mainly attributed to structural change (i.e. crystallization/melting) rather than heat dissipation from chains friction associated to viscoelasticity [40]. Regarding the square loading in figure1.c (for which the speed of loading is very high and should promote viscoelasticity), a mechanical hysteresis is recorded only when SIC takes place (i.e. for $\lambda_{max}>4$). With triangular loading, Figure 3b, the hysteresis (ΔW) is divided by 2 (between 0.001 and 1Hz) while the frequency is multiplied by 1000. This clearly demonstrates that the viscoelasticity is negligible in our experiments. Besides, the COP_{mat} [2,41], i.e. the ratio of the

heat that can be absorbed Q (approximated as being $Q = \rho * C_m * |\Delta T_2|$) divided by the mechanical hysteresis ΔW ($COP_{mat}=\frac{Q}{\Delta W}$), increases from 8 to 13 as λ_{min} decreases from 4 to 2 (Figure 4). But, as illustrated on Figure 4 where our results are compared to data obtained with Shape Memory Alloy [2], this increase is at the expense of the temperature variation (which strongly depends on the crystallinity variation).

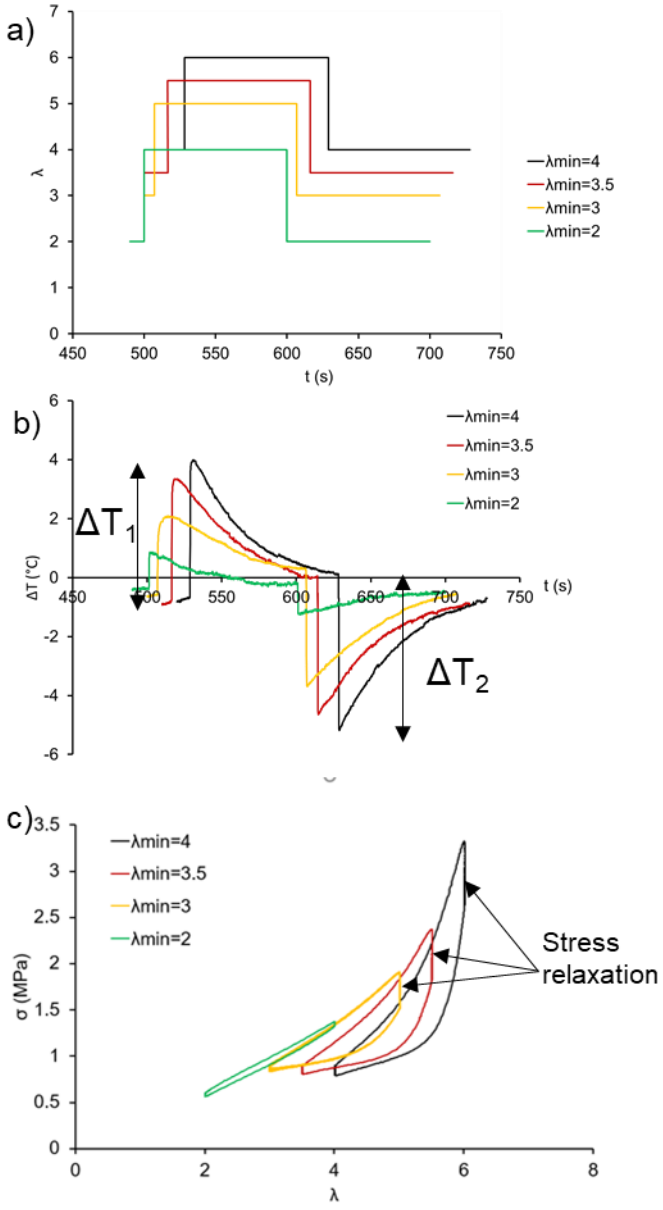

Figure1. $NR_{S1.46}$ under square wave solicitation at a frequency of f=0.005Hz for different λ_{min} (3rd and following cycles): (a) Extension ratio as a function of time (b) Resulting temperature variation (c) Stress-extension ratio curves

For mechanical cycles (4<λ<6), which previously leads to the largest$|\Delta T_2|$, we also studied the influence of the shape of loading (triangular and square) still with $NR_{S\_1.46}$, and at different

frequencies [0.001; 0.005; 0.01; 0.05; 0.1; 0.5; 1Hz]. The compared $|\Delta T|$ in both cycle types (see supporting information S1) are the difference between the temperature measured at the beginning of the unloading step (from λ_{max}), and the one measured at the end of this same step, i.e. when λ_{min} is reached. As shown in Figure 2, for the square cycles, $|\Delta T|$ (equal to $|\Delta T_2|$) decreases with the frequency increase. This is consistent with what we know from the crystallization kinetics after a sudden strain (supporting information S3): the longer the holding step, the larger the crystallinity which can then melt during the unloading step (see schemes in supporting S5 which describe the change of crystallinity versus the loading shape). The holding time $\frac{1}{2f}$, goes from 100s at 0.005 Hz to 500ms at 1Hz, this leads during the unloading step, to a $\Delta\chi$ varying from -10% to -5%. Both $\Delta\chi$ induce a temperature decrease of ca. 3.4°C and ca. 1.7°C respectively. These two values are consistent with the evolution of $|\Delta T|$ (observed in Figure 2: from 5.5°C at 0.005 Hz down to 4°Cat 1Hz) by taking into account the effect of entropic elasticity in addition to one of SIC. This means that the entropic elasticity contribution becomes predominant for frequency above 0.1 Hz.

With triangular cycle, $|\Delta T|$ shows a maximum at 0.01 Hz. This can be explained by a competition between the crystallization kinetics and the heat exchange of the material with its environment [42]. Decreasing the frequency promotes heat transfer which lowers the temperature variation (this one should tend towards 0 at very low frequency). At high frequencies, in spite of a negligible heat transfer, the temperature variation should also decrease because crystallization has less time to proceed [34] in the range of used frequencies. In addition, there is the contribution of entropic elasticity, which depends only on the variation in the extension ratio. This explains that the curve does not tends toward zero at high frequency. Regardless of the frequency, $|\Delta T|$ is always greater for square signal; this is expected since the time spent at maximum extension ratio λ_{max} for which the SIC kinetics is faster [10,43,44], is greater and the heat exchange during unloading is minimized. This difference between both types of cycle logically diminishes at high frequencies as the duration of the plateau of the square signal decreases to such an extent that both signals become almost similar.

Finally, the mechanical hysteresis (i.e. the work measured during one cycle), is reported for both cycle types at different frequencies on Figure 2b. At f=1 Hz, the hysteresis areas are almost equal. However, by decreasing the frequency to f=0.005Hz, ΔW increases by around 40% in triangular and 200% in square-wave. This difference is mainly related to the holding step in the square signal, which leads to more stress relaxation, in relation, as previously said, with an increase in the crystallinity.

In more practical view, for frequencies close to those used in refrigeration systems (f=0.1hz,) potential heat exchange Q, deduced from the ΔT variation, is ca. 6.2 MJ/m^3 for the triangular cycle and ca. 7.2 MJ/m^3 for the square one, and the mechanical work is 0.25 MJ/m^3 and 0.60 MJ/m^3 respectively. These results lead to COP_{mat} of 25 and 12 respectively. The former value rivals the best ones found for SMAs, and is very close to the one found with natural rubber tubes at the same frequency under trapezoidal solicitation in conditions of real cooling system [17].On the basis of all these results, it appears that square type cycles enable to maximize the exchangeable heat, whereas it seems more judicious to work with a triangular signal to increase the COP_{mat}.

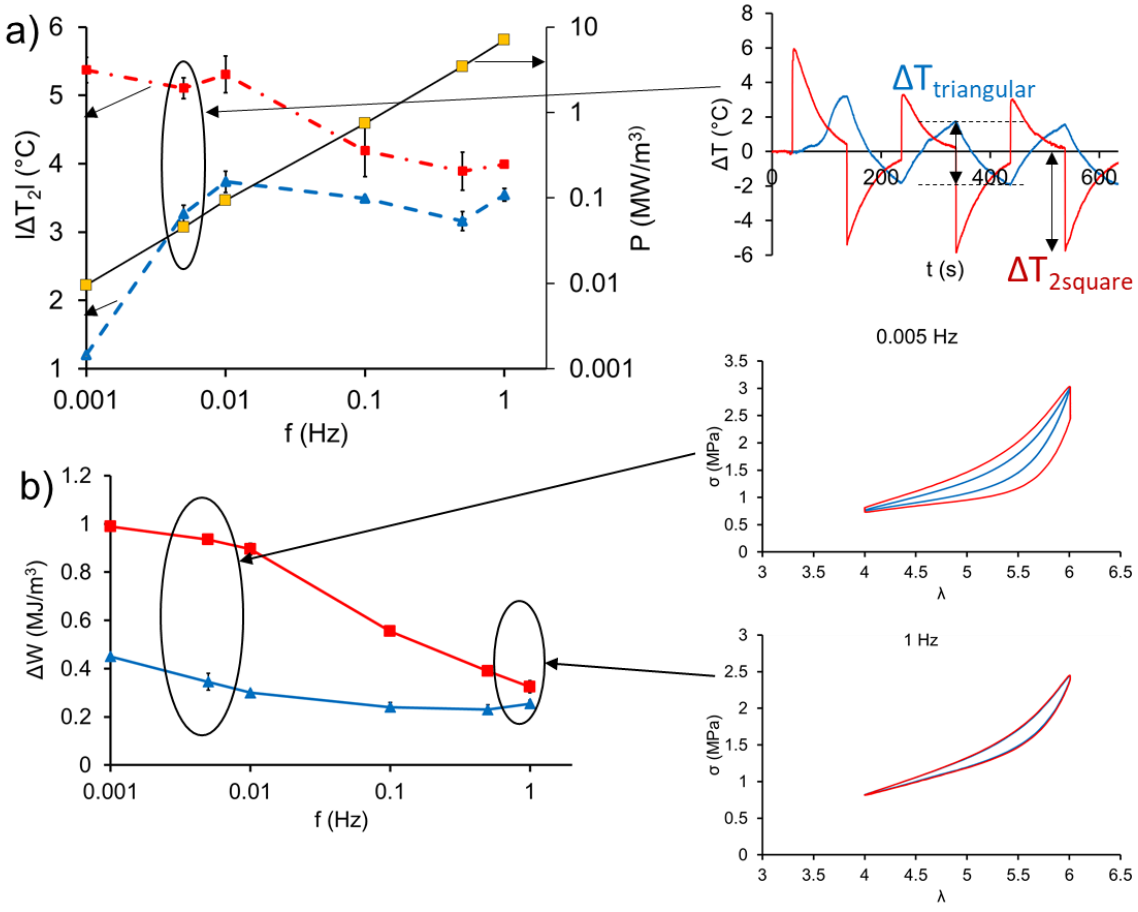

Figure.2 (a) Temperature variations during the unloading step measured for square (red) and triangular (blue) type solicitation, cooling power deduced from square signal measurement in yellow (b) Mechanical hysteresis deduced from the integration of the mechanical response over the whole cycle.

From the data obtained with the square signal, for which ΔT is obtained in adiabatic conditions, we may also calculate the maximum power P that can be used for solid refrigeration P. P can be estimated as $\rho * C_m * |\Delta T| * f$. As shown in Figure 2a it significantly increases with the frequency, despite the decrease of $|\Delta T_2|$. Thus, lowering the frequency of the cycle (in the range accessible for this experiment), in the hope that it will maximize crystallization, is not enough to compensate the reduce power. In this context, for a given material, optimization of the device's cooling power should focus on both heat exchange within the device and on crystallization kinetics. Thus, the frequency should not be increased above 10Hz because the ability of the material to crystallize may be greatly reduced (SIC kinetics do not have time to occur because the minimum time required to start crystallization is of the order of 100 ms) and because viscoelastic self-heating is known to increase significantly at high frequency[34].

We may now consider the impact of the material properties on the elastocaloric effect. We selected an extension ratio range of λ_{min}=3.5 to λ_{max}=5.5 due to the proximity of the extension ratio at break, equal to 6 for some formulations tested [27]. We chose a frequency of f=0.1 Hz as the temperature variation in the material can then be considered as adiabatic [17] and homogeneous. A triangular waveform was selected because it has been previously seen to yield the best COP_{mat}. Interestingly, as shown in Figure.3, among the NR samples studied, the more cross-linked the material, the greater the exchangeable heat Q and the mechanical hysteresis (to which it is strongly correlated). This results in a quasi-constant COP of the order of 25-30 while Q increases from 5 to 7.0 MJ/m^3. On the other hand, in the case of the peroxide-crosslinked SR, the heat that can be exchanged is very low (2.7 MJ/m^3) due to its lower ability to crystallize with extension ratio, but the mechanical hysteresis being rather low, this results in the highest COP (of the order of 30).

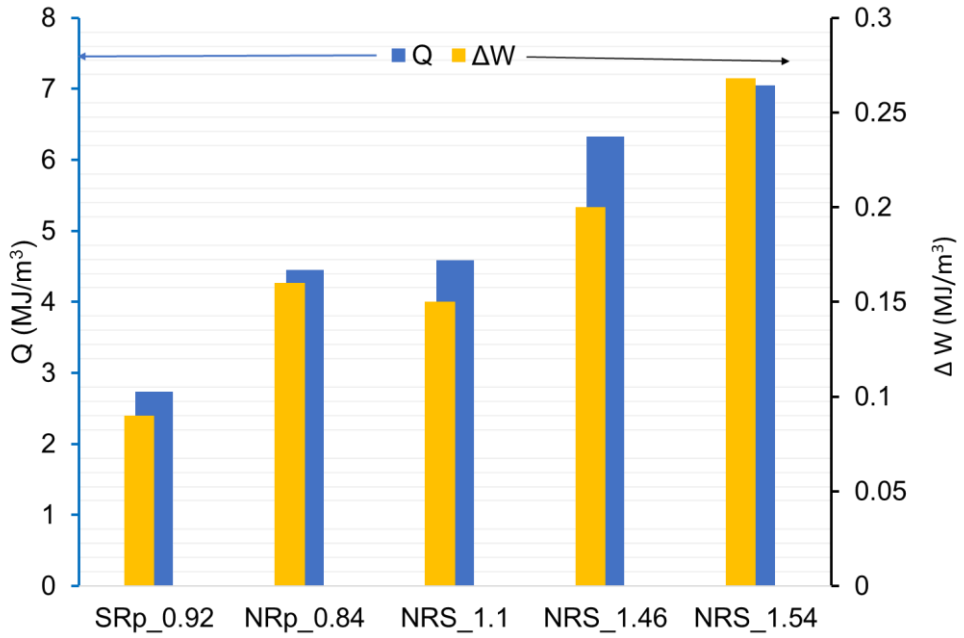

Figure.3 exchangeable heat Q and ΔW for cycles performed between λ=3.5 and λ=5.5 at f=0.1 Hz

All the COP_{mat} values deduced for the different studied materials have been reported on Figure 4 for comparison as a function of the temperature variation $|\Delta T|$.We have also painted an area in light blue which represents the domain of all the data that Chen et al. collected from the literature and added the data that they obtained in their study (black disks) with Shape Memory Alloys NiTi gradient-structured materials [2,45].

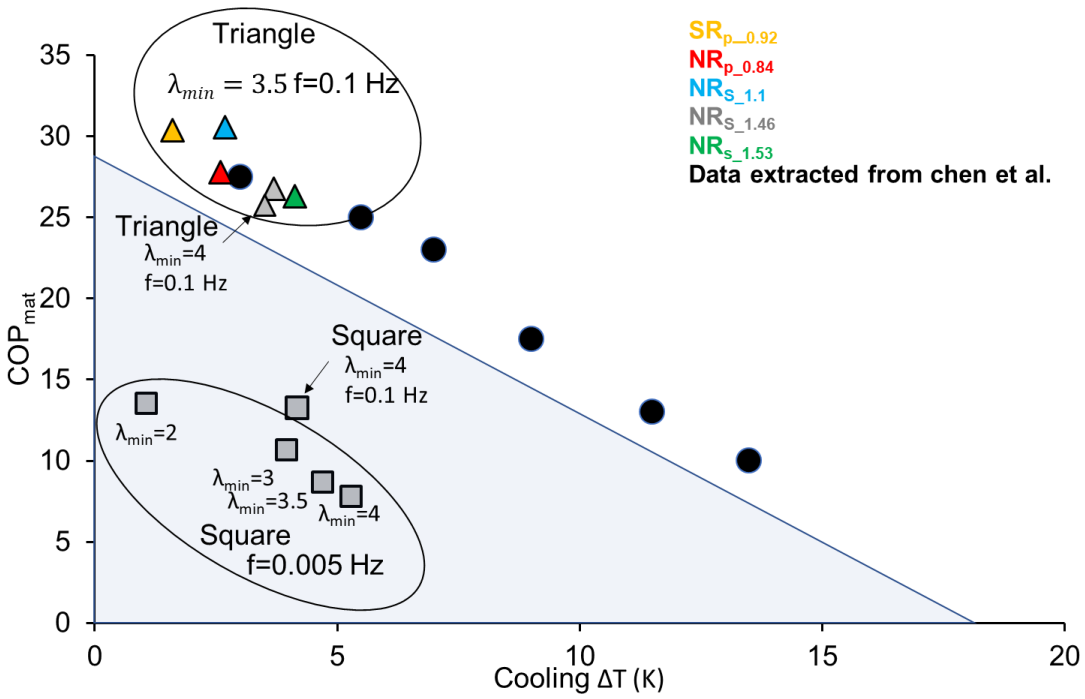

Figure. 4: COP_{mat} as a function of adiabatic cooling temperature for Shape Memory Alloys (SMA) and for our studied rubbers. Each color corresponds to a material formulation as specified in the figure legend. Square symbols are for square type cycles, triangle for triangular type cycles.

In terms of COP_{mat}, rubbers which do not have a great tendency to crystallize such as polyisoprene synthetic rubber [5] seem to be the best, while to maximize ΔT, the best of our formulations is NR crosslinked with sulfur and having a crosslink density close to 1.5×10^{-4} mol/cm^3. This material has a COP_{mat} of about 27 and enables a $\Delta T \approx 4K$. Its performance are comparable with those of the best SMA with temperature variation below 5 K and high COP (>25). It actually corresponds to the formulation with the best crystallization ability [3] combined with a large entropic elasticity. A higher cross-link density (above 1.6×10^{-4} mol/cm^3) could restrict strain at break and reduce crystallization and thus impede improved elastocaloric performance [27,46]. Conversely, a lower cross-linking density would diminish the elastocaloric effect by allowing stable crystals to persist at room temperature [31], as well as reducing the contribution of entropic elasticity [47].

4. Conclusions

To summarize, we have studied different critical parameters governing the eCe (elastocaloric effect) of poly-isoprene rubber NR and SR) in use conditions of a cooling device, i.e. under partial cyclic loading (the chosen amplitude of extension ratio was fixed to 2). As expected, we showed that the eCe increases when the mimimum pre-extension ratio is increased. Moreover, cycles must not be performed at too high frequency (above 1Hz) since it reduces SIC contribution to the exchangeable heat. It is not judicious either to cycle below 0.1Hz since it reduces too much the power of the cooling system. At intermediate frequency (0.1 Hz < f < 0.5Hz), often used in elastocaloric systems, the best thermal response is obtained with square type cycle since the holding step enables to maximize crystallization, whereas the rapid adiabatic unloading enables to maximize the temperature variation and therefore the exchangeable heat. Nevertheless, the stress relaxation obtained during the holding step also strongly increases the mechanical hysteresis, and therefore promotes energy waste. From this point of view, and without considering the way heat could be exchanged in the device (which may need a holding step), the triangular type signal seems finally the best option. Regarding the formulation, rubbers that do not have a great tendency to crystallise such as polyisoprene synthetic rubber seem to have the best COP_{mat}, while to maximise ΔT, the best of our formulations are NR crosslinked with sulphur and having a crosslink density close to 1.5×10^{-4} mol/cm^3, which combine large strain induced crystallisation and entropic elasticity. This material has a COP_{mat} of about 27 and allows a $\Delta T\approx4K$, i.e.performance comparable to that of the best Shape Memory Alloys (at equivalent COP_{mat}).

Acknowledgements

The authors thank the Agence Nationale pour la Recherche (ANR, France) for its financial support through the Project No. ECPOR (No. ANR-17-CE05-0016).

Data Availability

The data that support the findings of this study are available from the corresponding authors upon reasonable request.

References

[1] X. Moya, S. Kar-Narayan, N.D. Mathur, Caloric materials near ferroic phase transitions, Nat. Mater. 13 (2014) 439–450. https://doi.org/10.1038/nmat3951.

[2] J. Chen, L. Lei, G. Fang, Elastocaloric cooling of shape memory alloys: A review, Mater. Today Commun. 28 (2021) 102706. https://doi.org/10.1016/j.mtcomm.2021.102706.

[3] J. Chenal, L. Chazeau, L. Guy, Y. Bomal, C. Gauthier, Molecular weight between physical entanglements in natural rubber : A critical parameter during strain-induced crystallization, 48 (2007) 1042–1046. https://doi.org/10.1016/j.polymer.2006.12.031.

[4] S. Toki, B.S. Hsiao, Nature of Strain-Induced Structures in Natural and Synthetic Rubbers under Stretching, Macromolecules. 36 (2003) 5915–5917. https://doi.org/10.1021/ma034729e.

[5] E.M. N. Candau, L. Chazeau, Laurent; J-M Chenal, C. Gauthier, Compared abilities of natural (NR) and synthetic (IR) polyisoprene cis-1,4 to crystallize under strain at high strain rates, Phys. Chem. Chem. Phys. 18 (2016) 3472–3481. https://doi.org/10.1039/C5CP06383C.

[6] S.L. Dart, R.L. Anthony, E. Guth, Rise of Temperature on Fast Stretching of Synthetics and Natural Rubbers, Ind. Eng. Chem. 34 (1942) 1340–1342. https://doi.org/10.1021/ie50395a020.

[7] F. Greibich, R. Schwödiauer, G. Mao, D. Wirthl, M. Drack, R. Baumgartner, A. Kogler, J. Stadlbauer, S. Bauer, N. Arnold, M. Kaltenbrunner, Elastocaloric heat pump with specific cooling power of 20.9 W g–1 exploiting snap-through instability and strain-induced crystallization, Nat. Energy. 6 (2021) 260–267. https://doi.org/10.1038/s41560-020-00770-w.

[8] Z. Xie, G. Sebald, D. Guyomar, Comparison of elastocaloric effect of natural rubber with other caloric effects on different-scale cooling application cases, Appl. Therm. Eng. 111 (2017) 914–926. https://doi.org/10.1016/j.applthermaleng.2016.09.164.

[9] N. Candau, A. Zimny, E. Vives, M.L. Maspoch, Elastocaloric Waste/Natural Rubber Materials with Various Crosslink Densities, Polymers (Basel). 15 (2023) 2566. https://doi.org/10.3390/polym15112566.

[10] H. Haissoune, J.-M. Chenal, L. Chazeau, G. Sebald, I. Morfin, L. Lebrun, F. Dalmas, G. Coativy, Elastocaloric effect: Impact of heat transfer on strain-induced crystallization kinetics of natural rubber, Polymer (Guildf). 263 (2022) 125506. https://doi.org/10.1016/j.polymer.2022.125506.

[11] N. Candau, E. Vives, A.I. Fernández, M.L. Maspoch, Elastocaloric effect in vulcanized natural rubber and natural/wastes rubber blends, Polymer (Guildf). 236 (2021). https://doi.org/10.1016/j.polymer.2021.124309.

[12] A. Torello, E. Defay, Maximizing adiabatic temperature change in elastocaloric polymers, Chem. 8 (2022) 3165–3167. https://doi.org/10.1016/j.chempr.2022.11.017.

[13] G. Coativy, H. Haissoune, L. Seveyrat, G. Sebald, L. Chazeau, J.-M. Chenal, L. Lebrun, Elastocaloric properties of thermoplastic polyurethane, Appl. Phys. Lett. 117 (2020) 193903. https://doi.org/10.1063/5.0023520.

[14] S. Zhang, Y. Fu, C. Li, X. Nie, J. Chen, Y. Zhou, Z. Ye, X. Zhou, B. Shu, C. Xiong, Q. Yang, Q. Wang, Polymer elastomer near plastic-to-rubber critical transition produces enhanced elastocaloric effects, Cell Reports Phys. Sci. 3 (2022) 101147. https://doi.org/10.1016/j.xcrp.2022.101147.

[15] R. Bennacer, B. Liu, M. Yang, A. Chen, Refrigeration performance and the elastocaloric effect in natural and synthetic rubbers, Appl. Therm. Eng. 204 (2022) 117938. https://doi.org/10.1016/j.applthermaleng.2021.117938.

[16] K. Wang, K. Engelbrecht, C.R.H. Bahl, Additive manufactured thermoplastic elastomers for low-stress driven elastocaloric cooling, Appl. Mater. Today. 30 (2023) 101711. https://doi.org/10.1016/j.apmt.2022.101711.

[17] G. Sebald, G. Lombardi, G. Coativy, J. Jay, L. Lebrun, A. Komiya, High-performance polymer-based regenerative elastocaloric cooler, Appl. Therm. Eng. 223 (2023) 120016. https://doi.org/10.1016/j.applthermaleng.2023.120016.

[18] G. Sebald, A. Komiya, J. Jay, G. Coativy, L. Lebrun, Regenerative cooling using elastocaloric rubber: Analytical model and experiments, J. Appl. Phys. 127 (2020) 094903. https://doi.org/10.1063/1.5132361.

[19] G. Sebald, Z. Xie, D. Guyomar, Fatigue effect of elastocaloric properties in natural rubber, Philos. Trans. R. Soc. A Math. Phys. Eng. Sci. 374 (2016) 20150302.

https://doi.org/10.1098/rsta.2015.0302.

[20] Z. Xie, G. Sebald, D. Guyomar, Elastocaloric effect dependence on pre-elongation in natural rubber, Appl. Phys. Lett. 107 (2015). https://doi.org/10.1063/1.4929395.

[21] N. Candau, R. Laghmach, L. Chazeau, J.-M. Chenal, C. Gauthier, T. Biben, E. Munch, Strain-Induced Crystallization of Natural Rubber and Cross-Link Densities Heterogeneities, Macromolecules. 47 (2014) 5815–5824. https://doi.org/10.1021/ma5006843.

[22] Z. Xie, C. Wei, D. Guyomar, G. Sebald, Validity of Flory's model for describing equilibrium strain-induced crystallization (SIC) and thermal behavior in natural rubber, Polymer (Guildf). 103 (2016) 41–45. https://doi.org/10.1016/j.polymer.2016.09.038.

[23] S. Trabelsi, P.A. Albouy, J. Rault, Crystallization and melting processes in vulcanized stretched natural rubber, Macromolecules. 36 (2003) 7624–7639. https://doi.org/10.1021/ma030224c.

[24] N. Candau, L. Chazeau, J. Chenal, C. Gauthier, E. Munch, Complex dependence on the elastically active chains density of the strain induced crystallization of vulcanized natural rubbers , from low to high strain rate, Polymer (Guildf). 97 (2016) 158–166. https://doi.org/10.1016/j.polymer.2016.05.020.

[25] Z. Xie, G. Sebald, D. Guyomar, Elastocaloric effect dependence on pre-elongation in natural rubber, Appl. Phys. Lett. 107 (2015) 4–8. https://doi.org/10.1063/1.4929395.

[26] S. Amnuaypornsri, J. Sakdapipanich, S. Toki, B.S. Hsiao, N. Ichikawa, Y. Tanaka, Strain-induced crystallization of natural rubber: Effect of proteins and phospholipids, Rubber Chem. Technol. 81 (2008) 753–766. https://doi.org/10.5254/1.3548230.

[27] Y. Ikeda, Y. Yasuda, K. Hijikata, M. Tosaka, S. Kohjiya, Comparative study on strain-induced crystallization behavior of peroxide cross-linked and sulfur cross-linked natural rubber, Macromolecules. 41 (2008) 5876–5884. https://doi.org/10.1021/ma800144u.

[28] M. Tosaka, S. Oue, A. Gros, B. Huneau, E. Verron, S. Poompradub, Formation of Crystallites with Low Surface Energy, J. Fiber Sci. Technol. 74 (2018) 133–142. https://doi.org/10.2115/fiberst.2018-0019.

[29] A. Gros, B. Huneau, E. Verron, Derivation of the chain length distribution in

crosslinked elastomers from thermoporometric literature data, Thermochim. Acta. 718 (2022) 179383. https://doi.org/10.1016/j.tca.2022.179383.

[30] F. Katzenberg, B. Heuwers, J.C. Tiller, Superheated rubber for cold storage, Adv. Mater. 23 (2011) 1909–1911. https://doi.org/10.1002/adma.201100408.

[31] B. Heuwers, D. Quitmann, F. Katzenberg, J.C. Tiller, Stress-induced melting of crystals in natural rubber: A new way to tailor the transition temperature of shape memory polymers, Macromol. Rapid Commun. 33 (2012) 1517–1522. https://doi.org/10.1002/marc.201200313.

[32] P.J. Flory, J. Rehner, Statistical Mechanics of Cross-Linked Polymer Networks II. Swelling, J. Chem. Phys. 11 (1943) 521–526. https://doi.org/10.1063/1.1723792.

[33] R.F. Boyer, R.L. Miller, Correlations involving the Mooney—Rivlin C2 constant and the number of chain atoms between physical entanglements, Nc, Polymer (Guildf). 28 (1987) 399–407. https://doi.org/10.1016/0032-3861(87)90192-3.

[34] N. Candau, L. Chazeau, J.-M. Chenal, C. Gauthier, J. Ferreira, E. Munch, C. Rochas, Characteristic time of strain induced crystallization of crosslinked natural rubber, Polymer (Guildf). 53 (2012) 2540–2543. https://doi.org/10.1016/j.polymer.2012.04.027.

[35] P.-A. Albouy, G. Guillier, D. Petermann, A. Vieyres, O. Sanseau, P. Sotta, A stroboscopic X-ray apparatus for the study of the kinetics of strain-induced crystallization in natural rubber, Polymer (Guildf). 53 (2012) 3313–3324. https://doi.org/10.1016/j.polymer.2012.05.042.

[36] J.C. Mitchell, D.J. Meier, Rapid Stress-Induced Crystallization in Natural Rubber, Rubber Chem. Technol. 42 (1969) 1420–1432. https://doi.org/10.5254/1.3539309.

[37] N. Candau, E. Vives, A.I. Fernández, M.L. Maspoch, Elastocaloric effect in vulcanized natural rubber and natural/wastes rubber blends, Polymer (Guildf). 236 (2021) 124309. https://doi.org/10.1016/j.polymer.2021.124309.

[38] P.J. Flory, Thermodynamics of Crystallization in High Polymers. I. Crystallization Induced by Stretching, J. Chem. Phys. 15 (1947) 397–408. https://doi.org/10.1063/1.1746537.

[39] P. Sotta, P.-A. Albouy, Strain-Induced Crystallization in Natural Rubber: Flory's

Theory Revisited, Macromolecules. 53 (2020) 3097–3109. https://doi.org/10.1021/acs.macromol.0c00515.

[40] J.-B. Le Cam, Energy storage due to strain-induced crystallization in natural rubber: The physical origin of the mechanical hysteresis, Polymer (Guildf). 127 (2017) 166–173. https://doi.org/10.1016/j.polymer.2017.08.059.

[41] J. Cui, Y. Wu, J. Muehlbauer, Y. Hwang, R. Radermacher, S. Fackler, M. Wuttig, I. Takeuchi, Demonstration of high efficiency elastocaloric cooling with large ΔT using NiTi wires, Appl. Phys. Lett. 101 (2012) 073904. https://doi.org/10.1063/1.4746257.

[42] H. Haissoune, Etude de l'effet élastocalorique (eC) dans le Caoutchouc Naturel (NR) pour les systèmes de réfrigération solide, Thèse de doctorat, Lyon, INSA, 2022. https://theses.insa-lyon.fr/publication/2022LYSEI028/these.pdf

[43] P.-A. Albouy, P. Sotta, Draw Ratio at the Onset of Strain-Induced Crystallization in Cross-Linked Natural Rubber, Macromolecules. 53 (2020) 992–1000. https://doi.org/10.1021/acs.macromol.9b01957.

[44] K. Brüning, K. Schneider, S. V. Roth, G. Heinrich, Kinetics of strain-induced crystallization in natural rubber: A diffusion-controlled rate law, Polymer (Guildf). 72 (2015) 52–58. https://doi.org/10.1016/j.polymer.2015.07.011.

[45] J. Chen, L. Xing, G. Fang, L. Lei, W. Liu, Improved elastocaloric cooling performance in gradient-structured NiTi alloy processed by localized laser surface annealing, Acta Mater. 208 (2021) 116741. https://doi.org/10.1016/j.actamat.2021.116741.

[46] P. González Hernández, Luis; Rodríguez Díaz, Andrés; Valentín, Juan L. ; Marcos-Fernández, Ángel ; Posadas, Conventional and Efficient Crosslinking of Natural Rubber: Effect of Heterogeneities on the Physical Properties, Elastom. UND KUNSTSTOFFE. (2005) 638–643. http://hdl.handle.net/10261/34215.

[47] L.R.G. Treloar, The Elasticity and Related Properties of Rubbers, Rubber Chem. Technol. 47 (1974) 625–696. https://doi.org/10.5254/1.3540456.

452

453 Graphical abstract

454

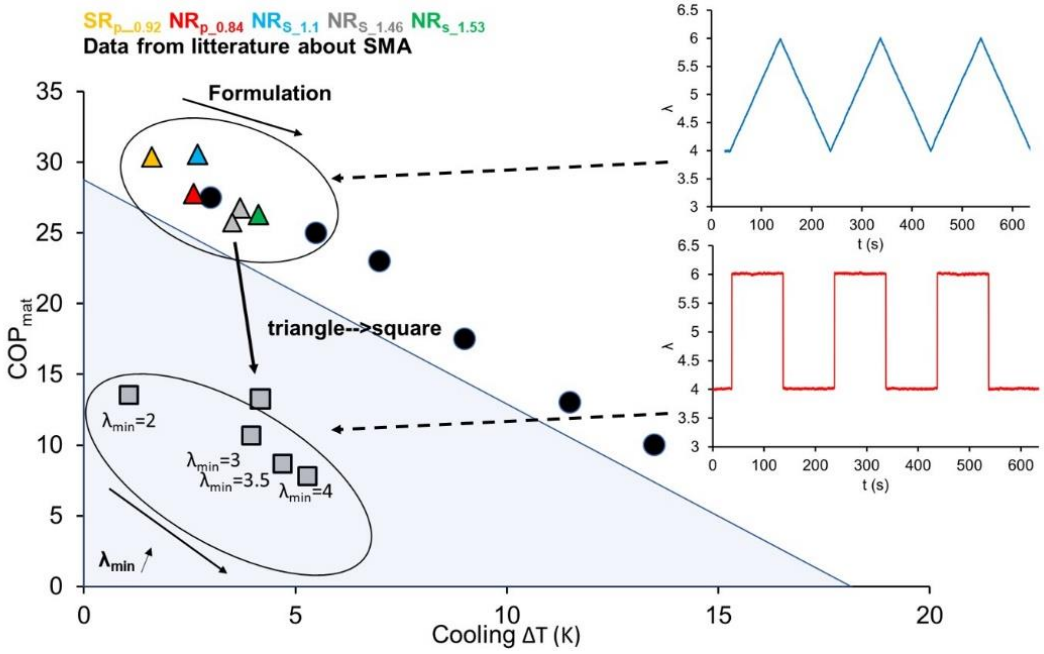

455

456